Transketolases from animals are structurally different from others

Numa Georges [a], Lionel Ballut [b], Guillaume Octobre [a], Nushin Aghajari [b], Laurence Hecquet [c], Franck Charmantray [c], **Bastien Doumèche** [a*]
[a] Univ Lyon, Université Claude Bernard Lyon 1, CNRS, ICBMS UMR5246, 69622 Villeurbanne, France
[b] Molecular Microbiology and Structural Biochemistry, UMR 5086, CNRS-Université de Lyon, F-69367 Lyon, France
[c] Université Clermont Auvergne, CNRS, SIGMA Clermont, Institut de Chimie de Clermont-Ferrand (ICCF) F-63000 Clermont-Ferrand (France)

E-mail of corresponding author: **doumeche@univ-lyon1.fr**

Why Transketolases ?

Transketolase (TKs, EC 2.2.1.1) is a key enzyme of the pentose-phosphate pathway (PPP) controlling 70% of its activity. As the the PPP is linked to several other crucial pathways (glycolysis, synthesis of nucleotides, NADPH, and amino acids) as well as in regulating oxidative stress, it is an interresting target for antimicrobial drugs. This could only be effective if Human TK is significantly different from TKs of pathogens to avoid being inhibited by the drug.

Here, we compare the structure of Human TK and those of 14 priority pathogen from the WHO lists through molecular modelling, enzyme expression and kinetic characterization, as well as resolving structures by X-ray crystallography for some of them.

TK in the Evolution

The reviewed sequences of 30 TKs from animals, plants, bacteria, yeasts, and parasites are aligned using Clustal ω and a dendrogram is constructed (1). TKs organize into two groups based on their average size and then into sub-groups based on their clade. Group I includes plants, bacteria (divided into three subgroups), yeasts, and most parasites, while group II consist of *Schistosoma sp.* and animals. The latters are 27 (+/-2) residues shorter than TKs from group I, corresponding to a shorter length of linker I (see further).

1

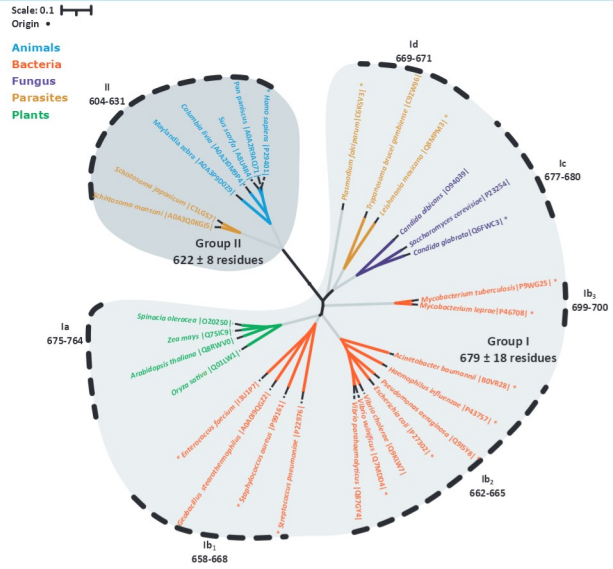

Enzyme kinetics

In the PPP, TKs catalyze the reversible transfert of a two-carbon units from a phosphorylated ketose donor to a phosphorylated aldose acceptor forming transiently α,β-dihydroxyethylthiamine pyrophosphate (DHETPP) (2A). An assay based on the oxidation of the DHETPP intermediate by $Fe(CN)_6^{3-}$ (ε_M^{420nm} = 1000 $M^{-1}.cm^{-1}$) using *D*-fructose-6-phosphate as the ketose is used to determine apparent kinetic parameters (2B). Kinetic constants of 11 TKs from pathogens have values in the same range, while *hs*TK presents higher K_M values for F6P and $Fe(CN)_6^{3-}$ as well as a lower k_{cat} value in this assay. This reflects the specialization of *hs*TK during evolution and its uniqueness.

2A *Reaction catalyzed in the PPP by TK*

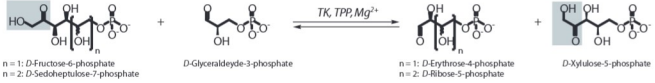

2B *Enzymatic assay*

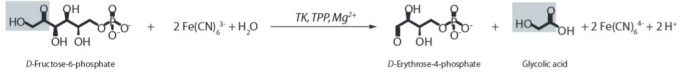

TK	K_{F6P}^{app} (μM)	$K_{Fe(CN)6}^{app}$ (μM)	k_{cat} (s^{-1})
Pathogen TKs (range value)	78-298	254-1069	0.14-1.68
*hs*TK	443.9 ± 17.6	1385.2 ± 9.2	0.06 ± 0.01

Rates were obtained in 50 mM HEPES buffer pH 7.0, 100 mM KCl, 2 mM $MgCl_2$, pH 7.0 at 37°C containing 0-500 μM F6P, 0-200 μM $Fe(CN)_6^{3-}$, and 0-200 μM TPP (n = 3). Only one substrate concentration is varied for the determination of the Michaelis-Menten constants, the others being at maximal concentration.

TKs expressed in this work

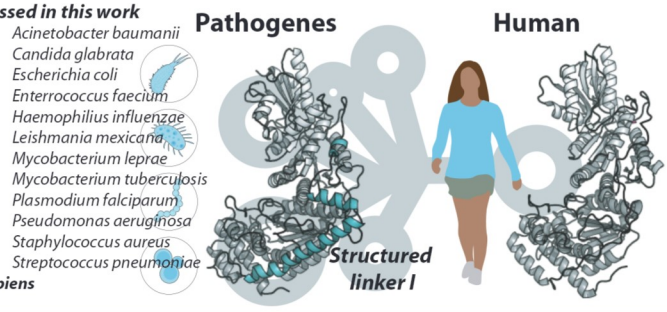

TK structure

TKs are conserved, nested V-shaped homodimers with two TPP cofactors localized between the pyridinium (Pyr) domain of one monomer and the pyrophosphate (PP) domain of the other (3A). The third domain (C-ter) is involved in the dimer stabilization. Pyr and PP domains are connected by linker I. The six new structures of TK (*ef*TK 8R3P, *hi*TK 8R3O, *pf*TK 8R3Q, *sa*TK 8R3S, *sp*TK 8R3R, *vv*TK 8QMF) share this fold. The TPP binding site formed by 78-82 residues is conserved always presenting six histidyl, one glutamyl and one aspartyl residues (3C). In *hs*TK, this binding site presents 33 residues never found in any other TK and a glutamyl residue in place of one the histidyl residue. On the contrary, the monomer-monomer interface is highly variable with only a few conserved residues (3B). Linker I of *hs*TK is shorter (40 residues) without secondary structures compared to TKs from pathogens that are all longer (77+/-2 residues) and are all forming α-helices. This fold defines a cavity suspected to be a cooperative inhibitor binding site (shown by enzyme kinetics and docking) (3D, 3E).

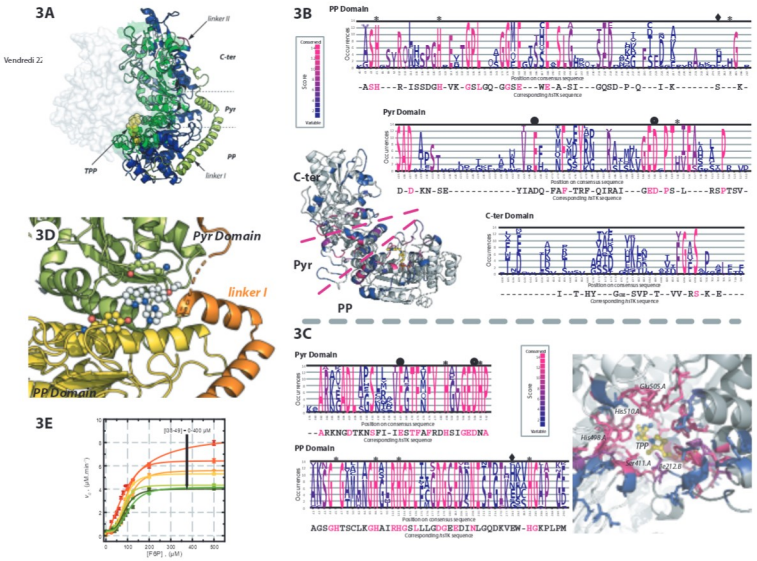

Structure of dimeric TK from *Vibrio vulificus* (8QMF) as represnetative structure of TKs (A). Monomer interface mapping (B) and homodimer active site mapping (B) of the 14 TKs. Logos show residue occurrences for each consensus position with scores from dark blue (variable residues) to pink (conserved residues). The *hs*TK sequence is aligned below the logos and identical residues to those having a score ≥12 are colored in pink. Residues of the histidine crown (*), His 281 (◊), Glu 447 initiating TPP activation (•), and Asp 506 stabilizing the thiazolium ring of TPP (°) are indicated. If no residues are shown on the logos, this indicates that only *hs*TK has a residue at this spatial position. Residues are projected onto the monomeric (B) or dimeric (C) structure of a consensus TK model (white or white and grey ribbons, respectively) using the same color as for the logos. TPP is represented by balls and sticks (carbon is yellow, nitrogen blue, oxygen red, phosphorus orange). The three domains are separated by pink dotted lines (B). Some conserved residues are also shown as sticks and labelled for ease of orientation (B). Molecular docking of inhibitor I38-49 on *vv*TK showing its position on the cavity delimitated by linker I in TK from pathogens (group I, 3D) and evidence of cooperative behavior induced by increasing concentrations of I38-49 (3E)

Conclusion

Transketolases from pathogens (group I) and from humans (group II) have similar active sites but different interfaces and different linker I (between PP and Pyr domains). This leads to the formation of a cavity in TKs of group I (absent in TKs of group II), suspected to be a cooperative binding site for inhibitors. This supports the idea that inhibitors of TK from pathogens targeting this site will be ineffective on human TK and will be suitable antimicrobial drugs.

Acknowledgment & Funding Sources

The Project **CEITOP (Criblage Electrochimique d'Inhibiteur de Transcétolases d'Organismes Pathogènes)** is funded by the Region Auvergne-Rhone-Alpes (AuRA). The AuRA region is greatly acknowledged for the funding of one of us (R.-N. G.). The authors thank the SOLEIL synchrotron for access to beamline PROXIMA-2A and the European Synchrotron Radiation Facility for access to MX-beamlines. Technical support from all the beamlines staff is gratefully acknowledged.

La Région Auvergne-Rhône-Alpes

References: Georges et al., *Biochemistry*, **2024**, doi: 10.1021/acs.biochem.3c00714 ; Georges et al., *Protein Science*, **2024**, 33 : e4884, doi: 10.1002/pro.4884; Fullam et al., *Open Biology*, **2012**, 2(1), 110026, doi: 10.1098/rsob.110026 ; Lindqvist et al., *The EMBO Journal*, **1992**, 11(7), 2373, doi: 10.1002/j.1460-2075.1992.tb05301.x